

RNA Cleavage by a DNA Enzyme with Extended Chemical Functionality

Stephen W. Santoro,[†] Gerald F. Joyce,^{*,†} Kandasamy Sakthivel,[‡]
Svetlana Gramatikova,[‡] and Carlos F. Barbas, III^{*,‡}

Contribution from the Departments of Chemistry and Molecular Biology and the Skaggs Institute for Chemical Biology, The Scripps Research Institute, 10550 North Torrey Pines Road, La Jolla, California 92037, and the Department of Molecular Biology and the Skaggs Institute for Chemical Biology, The Scripps Research Institute, 10550 North Torrey Pines Road, La Jolla, California 92037

Received October 14, 1999

Abstract: In vitro selection techniques were applied to the development of a DNA enzyme that contains three catalytically essential imidazole groups and catalyzes the cleavage of RNA substrates. Nucleic acid libraries for selection were constructed by polymerase-catalyzed incorporation of C5-imidazole-functionalized deoxyuridine in place of thymidine. Chemical synthesis was used to define a minimized catalytic domain composed of only 12 residues. The catalytic domain forms a compact hairpin structure that displays the three imidazole-containing residues. The enzyme can be made to cleave RNAs of almost any sequence by simple alteration of the two substrate-recognition domains that surround the catalytic domain. The enzyme operates with multiple turnover in the presence of micromolar concentrations of Zn²⁺, exhibiting saturation kinetics and a catalytic rate of >1 min⁻¹. The imidazole-containing DNA enzyme, one of the smallest known nucleic acid enzymes, combines the substrate-recognition properties of nucleic acid enzymes and the chemical functionality of protein enzymes in a molecule that is small, yet versatile and catalytically efficient.

Introduction

Proteins and nucleic acids each have properties that offer unique advantages in performing catalytic transformations.¹ Proteins possess a wide variety of functional groups that are suited to a broad range of chemical tasks, enabling protein enzymes to achieve extraordinary catalytic rate enhancements. Pancreatic ribonuclease A (RNase A), for example, catalyzes the cleavage of a dinucleotide substrate with a turnover rate of 1400 s⁻¹ (ref 2). Nucleic acids, although not endowed with the functional diversity of protein enzymes, are uniquely suited for sequence-specific recognition of nucleic acids through Watson–Crick base pairing. This capability allows nucleic acid enzymes to carry out chemical transformations on nucleic acid substrates with high sequence specificity and catalytic efficiency. In addition, the substrate-recognition domains of some nucleic acid enzymes can be altered without disrupting catalytic activity, allowing them to operate in a general-purpose manner with nucleic acid substrates of almost any desired sequence.

Although nucleic acids do not contain diverse functional groups, their functional capabilities can be supplemented through the use of various metal and small-molecule cofactors. The activity of nearly all known nucleic acid enzymes is either dependent upon or greatly enhanced by divalent metal cations. In most cases, the metal is thought to participate directly in

catalysis.^{3–6} In some cases, however, the metal appears to play an indirect role, perhaps by increasing positive charge density within the active site or contributing to the structural integrity of the enzyme.^{7–11} One in vitro-selected DNA enzyme operates without divalent metals in the presence of millimolar concentrations of histidine. The histidine cofactor is thought to serve as a general base in promoting the cleavage of an RNA phosphodiester.¹² The development of this catalyst suggests that nucleic acid enzymes could be made to utilize a wide variety of small-molecule cofactors, greatly expanding their functional capacity.

The selection of nucleic acid catalysts that contain extended chemical functionality already built into the molecule has been made possible by the synthesis of functionalized NTP analogues that are efficiently incorporated by polymerases. Replacement of UTP by C5-substituted UTP analogues enabled the in vitro selection of an imidazole-containing RNA enzyme that catalyzes amide bond formation,¹³ and a pyridine-functionalized RNA enzyme that catalyzes a Diels–Alder cycloaddition reaction.¹⁴

(3) Yarus, M. *FASEB J.* **1993**, *7*, 31–39.

(4) Steitz, T. A.; Steitz, J. A. *Proc. Natl. Acad. Sci. U.S.A.* **1993**, *90*, 6498–6502.

(5) Pyle, A. M. *Science* **1993**, *261*, 709–714.

(6) Joyce, G. F. *Proc. Natl. Acad. Sci. U.S.A.* **1998**, *95*, 5845–5847.

(7) Hampel, A.; Cowan, J. A. *Chem. Biol.* **1997**, *4*, 513–517.

(8) Nesbitt, S.; Hegg, L. A.; Fedor, M. J. *Chem. Biol.* **1997**, *4*, 619–630.

(9) Young, K. J.; Gill, F.; Grasby, J. A. *Nucleic Acids Res.* **1997**, *25*, 3760–3766.

(10) Suga, H.; Cowan, J. A.; Szostak, J. W. *Biochemistry* **1998**, *37*, 10118–10125.

(11) Murray, J. B.; Seyhan, A. A.; Walter, N. G.; Burke, J. M.; Scott, W. G. *Chem. Biol.* **1998**, *5*, 587–595.

(12) Roth, A.; Breaker, R. R. *Proc. Natl. Acad. Sci. U.S.A.* **1998**, *95*, 6027–6031.

(13) Wiegand, T. W.; Janssen, R. C.; Eaton, B. E. *Chem. Biol.* **1997**, *4*, 675–683.

* Corresponding authors. Gerald F. Joyce: Telephone: (858) 784-9844. Fax: (858) 784-2943. E-mail: gjoyce@scripps.edu. Carlos F. Barbas, III: Telephone: (858) 784-9098. Fax: (858) 784-2583. E-mail: carlos@scripps.edu.

[†] Departments of Chemistry and Molecular Biology and the Skaggs Institute for Chemical Biology.

[‡] Department of Molecular Biology and the Skaggs Institute for Chemical Biology.

(1) Narlikar, G. J.; Herschlag, D. *Annu. Rev. Biochem.* **1997**, *66*, 19–59.

(2) delCardayré, S. B.; Raines, R. T. *Biochemistry* **1994**, *33*, 6031–6037.

Both the amide synthase and Diels–Alderase ribozymes require the functionally enhanced nucleotides for their catalytic activity, although the number of these nucleotides that are required and the role that they play in catalysis have not been defined.

Some naturally occurring RNA enzymes that have the ability to cleave RNA in a sequence-specific manner have been used as “catalytic antisense” agents to cleave target RNAs, both *in vitro* and *in vivo*.^{15,16} The *in vitro* evolution of RNA-cleaving DNA enzymes demonstrated that DNA might be applied in a similar capacity.^{17,18} Compared to analogous RNA enzymes, DNA enzymes are easier to prepare, more resistant to chemical and enzymatic degradation and, in some cases, have more favorable kinetic properties.¹⁹ DNA enzymes have been used to cleave a variety of target RNAs, both *in vitro*^{20,21} and *in vivo*.^{22–25}

The lack of a 2'-hydroxyl in DNA compared to its presence in RNA does not appear to be an impediment to efficient catalytic activity. It is intriguing to speculate how the catalytic ability of DNA might be enhanced if it were provided with some of the chemical groups that occur in proteins. The development of a family of dNTP analogues that can be incorporated efficiently into DNA by a polymerase²⁶ has made it possible to address this question experimentally. In the present study, functionally enhanced DNAs that contained C5-imidazole deoxyuridine residues (Figure 1) were directed to cleave a target RNA substrate, withholding high concentrations of divalent metal cations and instead providing micromolar concentrations of Zn²⁺. An imidazole moiety was chosen to provide the same chemical functionality that occurs in the amino acid histidine. Histidine residues are known to play a prominent role in the catalytic mechanism of many protein enzymes, including ribonucleases and other phosphoesterases.^{27,28} The Zn²⁺ cofactor was chosen because of its propensity to coordinate to imidazole nitrogens in either a structural or functional capacity. The resulting imidazole-containing DNA enzyme is a small, but highly efficient, general-purpose endoribonuclease. It provides an experimental demonstration of a DNA enzyme that embodies the chemical functionality of a protein enzyme.

Experimental Section

In Vitro Selection. An initial library was generated by template-directed extension of 2 nmol of 5'-biotin-d(GGAAAAA)r(GUAAC-UAGAGAU)d(GGAAGAGATGGCGAC)-3' on 3 nmol of 5'-GTGCCAAGCTTACCG-N₅₀-GTCGCCATCTCTCC-3' (N = G, A, T, or C) in a 1-mL reaction mixture containing 10 units μL⁻¹ Superscript II

(14) Tarasow, T. W.; Tarasow, S. L.; Eaton, B. E. *Nature* **1997**, *389*, 54–57.

(15) Christoffersen, R. E.; Marr, J. J. *J. Med. Chem.* **1995**, *38*, 2023–2037.

(16) Rossi, J. J. *Biodrugs* **1998**, *9*, 1–10.

(17) Breaker, R. R.; Joyce, G. F. *Chem. Biol.* **1994**, *1*, 223–229.

(18) Santoro, S. W.; Joyce, G. F. *Proc. Natl. Acad. Sci. U.S.A.* **1997**, *94*, 4262–4266.

(19) Santoro, S. W.; Joyce, G. F. *Biochemistry* **1998**, *37*, 13330–13342.

(20) Unrau, P. J.; Bartel, D. P. *Nature* **1998**, *395*, 260–263.

(21) Pyle, A. M.; Chu, V. T.; Jankowski, E.; Boudvillain, M. *Methods Enzymol.* **2000**, *317*, 140–146.

(22) Warashina, M.; Kuwabara, T.; Nakamatsu, Y.; Taira, K. *Chem. Biol.* **1999**, *6*, 237–250.

(23) Sun, L.; Cairns, M. J.; Gerlach, W. L.; Witherington, C.; Wang, L.; King, A. *J. Biol. Chem.* **1999**, *274*, 17236–17241.

(24) Zhang, X.; Xu, Y.; Ling, H.; Hattori, T. *FEBS Lett.* **1999**, *458*, 151–156.

(25) Wu, Y.; Yu, L.; McMahon, R.; Rossi, J.; Forman, S. J.; Snyder, D. S. *Hum. Gene Ther.* **1999**, *10*, 2847–2857.

(26) Sakthivel, K.; Barbas, C. F. *Angew. Chem., Int. Ed.* **1998**, *37*, 2872–2875.

(27) Gerlt, J. A. *Nucleases*, 2nd ed.; Cold Spring Harbor Laboratory Press: Plainview, 1993; pp 1–34.

(28) Lipscomb, W. N.; Sträter, N. *Chem. Rev.* **1996**, *96*, 2375–2433.

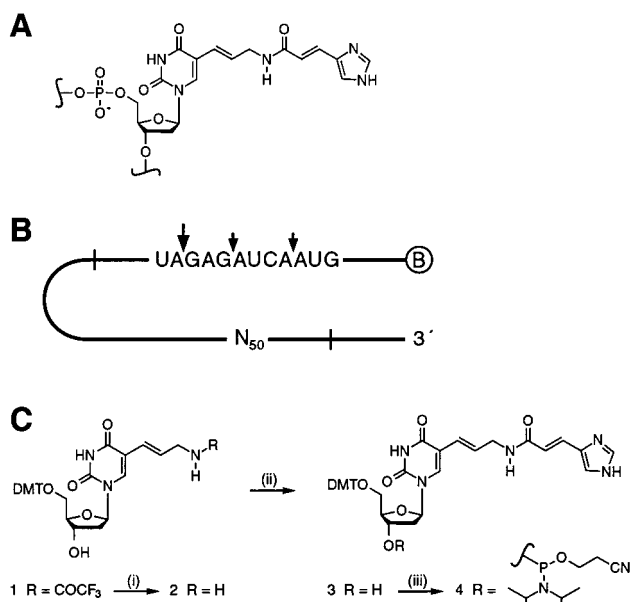


Figure 1. Compounds employed in the development and characterization of imidazole-functionalized RNA-cleaving DNAs. (A) Chemical structure of the C5-imidazole-deoxyuridine analogue that was incorporated in place of thymidine. The 4-imidazoleacrylic acid moiety is joined by an amide bond to the primary amine of 5-(3-aminopropyl)-deoxyuridine. (B) Library of imidazole-containing DNA molecules. Each molecule contained a 5'-biotin (encircled B), 12 target ribonucleotides (sequence shown), and 50 random-sequence deoxynucleotides (N₅₀). The selected molecules promoted phosphoester cleavage at one of three positions within the RNA region (arrows). After 16 rounds of selection, the molecules cleaved only at the position indicated by the large arrow. (C) Preparation of phosphoramidite **4**, involving the successive treatment of **1** with (i) aqueous ammonia in methanol, (ii) the *N*-hydroxysuccinimidyl ester of 4-imidazoleacrylic acid, and (iii) 2-cyanoethyl-*N,N*-diisopropylchlorophosphoramidite and *N,N*-diisopropylethylamine (see Materials and Methods).

reverse transcriptase (Life Technologies, Gaithersburg, MD), 3 mM MgCl₂, 75 mM KCl, 50 mM tris(hydroxymethyl)-aminomethane (Tris, pH 8.3), and 0.25 mM each of dATP, dCTP, dGTP, and the imidazole-functionalized dUTP analogue.²⁶ The conditions of the extension reaction were as previously described.¹⁸ Extension products were purified by non-denaturing polyacrylamide gel electrophoresis (PAGE).

The purified extension products (900 μL, ~1 nmol) were added to a 300-μL solution containing 600 mM NaCl, 0.4 mM Na₂EDTA, and 200 mM *N*-(2-hydroxyethyl)-piperazine-*N'*-3-propanesulfonic acid (EPPS; pH 7.0) and immobilized on an affinity column containing 200 μL of UltraLink Immobilized Streptavidin PLUS gel (Pierce, Rockford, IL), that had previously been equilibrated with three 200-μL volumes of wash buffer [150 mM NaCl, 0.1 mM Na₂EDTA, and 50 mM EPPS (pH 7.0)]. Following immobilization, the column was rinsed with five 200-μL volumes of wash buffer, five 200-μL volumes of ice-cold 0.1 N NaOH/150 mM NaCl, and five 200-μL volumes of wash buffer at 37 °C and then eluted at 37 °C over 1 h with three 200-μL aliquots of reaction buffer [10 μM Zn²⁺, 2 mM MgCl₂, 150 mM NaCl, 50 mM EPPS (pH 7.5)]. Eluted molecules were ethanol-precipitated in the presence of 100 pmols each of the primers, 5'-biotin-GGAAGAGATGGCGAC-3' and 5'-GTGCCAAGCTTACCG-3', and PCR-amplified in a 400-μL volume.²⁹

The PCR products were brought to a final NaCl concentration of 150 mM, immobilized as above on a column containing 50 μL of the streptavidin gel, rinsed with five 100-μL volumes of wash buffer, and eluted with two 40-μL volumes of 0.1 N NaOH/150 mM NaCl to recover the non-biotinylated strand. The isolated DNAs were ethanol-precipitated and used as templates in a primer extension reaction to begin the next round of *in vitro* selection. Rounds 2–10 were carried

(29) Breaker, R. R.; Joyce, G. F. *Chem. Biol.* **1995**, *2*, 655–660.

out as above except that the reaction scale was reduced 20-fold during the extension step and 4-fold during PCR and the reaction times were reduced to 30 min for round 8 and 1 min for rounds 9 and 10.

Beginning with the population of molecules obtained following the 10th round of selection, random mutations were introduced by hypermutagenic PCR.³⁰ Libraries were constructed from both mutagenized and non-mutagenized DNA templates by extension of an all-RNA primer, 5'-GGAAAAAGUAACUAGAGAUGGAAGAGAUG-GCGAC-3', using reverse transcriptase as a DNA-dependent DNA polymerase. Single-stranded molecules were isolated by immobilizing the extension products on streptavidin columns as described above, rinsing with five 100- μ L volumes of wash buffer, incubating in a 40- μ L solution containing 8 M urea, 0.1 mM Na₂EDTA, and 50 mM EPPS (pH 7.0) at 90 °C for 2 min, and eluting from the column, followed by ethanol precipitation. The recovered molecules were resuspended in 15 μ L of H₂O, preincubated at 37 °C for 5 min, and allowed to react at 37 °C following addition of 5 μ L of a 4 \times reaction buffer containing either 4 or 40 μ M Zn²⁺, 4 mM Mg²⁺, 600 mM Na⁺, and 200 mM EPPS (pH 7.0). Reaction times were decreased from 1 min for round 11 to 10 s for round 16. Reacted molecules were isolated by PAGE in a 10% denaturing gel, eluted from the gel, and amplified by asymmetric PCR to begin the next round of selection.

Intramolecular Cleavage Assays. Full-length precursor molecules corresponding to cloned individuals obtained following the 16th round of selection were prepared as described above for the populations after rounds 11–16. Cleavage was carried out at 37 °C following addition of 4 \times reaction buffer and was quenched by addition of an equal volume of a mixture containing 8 M urea, 20% sucrose, 90 mM Tris-borate (pH 8.3), 10 mM Na₂EDTA, and 0.1% SDS. Reaction products were separated by PAGE in a 20% denaturing gel and analyzed using a Molecular Dynamics PhosphorImager.

Synthesis of Imidazole-Functionalized Deoxyuridine Phosphoramidite (Figure 1C). 5'-O-DMT-5-(3-trifluoroacetylaminopropenyl)-2'-deoxyuridine (**1**; 680 mg, 1 mmol)^{26,31} was treated with 5 mL of aqueous ammonia in methanol at room temperature for 24 h. The reaction mixture was lyophilized, and the remaining residue (ninhydrin positive) was purified by silica gel column chromatography (0.1% triethylamine in 80:20 dichloromethane/methanol) to give **2** (510 mg, 87% yield). Compound **2** (500 mg, 0.85 mmol) was reacted with the *N*-hydroxysuccinimide ester of 4-imidazoleacrylic acid (235 mg, 1 mmol) in DMF at room temperature for 6 h. The reaction mixture was evaporated to dryness, and the residue was purified by silica gel column chromatography to give compound **3** (535 mg, 89% yield). ¹H NMR (400 MHz, CDCl₃ + CD₃OD) δ 7.72 (s, 1H), 7.64 (s, 1H), 7.34–7.11 (m, 11H), 6.77–6.74 (m, 4H), 6.36–6.16 (m, 3H), 5.51 (d, *J* = 24 Hz, 1H), 4.35 (m, 1H), 3.91 (s, 1H), 3.65 (s, 6H), 3.55 (d, *J* = 12 Hz, 2H), 3.26 (m, 2H), 2.45 (m, 2H). ¹³C NMR (CDCl₃ + DMSO-*d*₆) δ 165.99, 161.64, 157.59, 148.79, 143.4, 136.13, 135.89, 134.36, 134.2, 129.67, 128.75, 126.78, 126.5, 125.59, 121.94, 116.75, 111.76, 110.09, 109.09, 85.42, 85.28, 84.04, 70.01, 62.25, 53.29, 40.69, 39.08. HRMS calculated for C₃₉H₃₉N₅O₈ + Cs⁺: 838.1853; found: 838.1832. 2-Cyanoethyl-*N,N*-diisopropylchloro-phosphoramidite (0.23 mL, 1.28 mmol) was added to a solution of **3** (500 mg, 0.70 mmol) in dichloromethane containing *N,N*-diisopropylethylamine (0.18 mL, 1 mmol). The reaction mixture was stirred at room temperature for 30 min and then diluted with chloroform, washed with an aqueous solution of saturated sodium bicarbonate, dried with anhydrous sodium sulfate, and evaporated to dryness. The residue was purified by silica gel column chromatography to give phosphoramidite **4** (480 mg, 76% yield). HRMS calculated for C₄₈H₅₆N₇O₉P + Cs⁺: 1038.2931; found: 1038.2964. ³¹P NMR (CDCl₃) δ 149.16, 149.47.

Chemical Synthesis of Substrates and Enzymes. RNA substrates were prepared by chemical synthesis and deprotected as described previously.³² Deprotected substrates were purified by denaturing PAGE.

(30) Vartanian, J.; Henry, M.; Wain-Hobson, S. *Nucleic Acids Res.* **1996**, *24*, 2627–2631.

(31) Cook, A. F.; Vuocolo, E.; Brakel, C. L. *Nucleic Acids Res.* **1988**, *16*, 4077–4095.

(32) Wincott, F.; DiRenzo, A.; Shaffer, C.; Grimm, S.; Tracz, D.; Workman, C.; Sweedler, D.; Gonzalez, C.; Scaringe, S.; Usman, N. *Nucleic Acids Res.* **1995**, *23*, 2677–2684.

Imidazole-containing DNA enzymes were synthesized by using a Pharmacia Gene Assembler Special automated DNA/RNA synthesizer, employing phosphoramidite **4** with a coupling time of 5 min. The imidazole-functionalized DNA enzymes were deprotected according to standard protocols, desalted by using a NAP-5 column (Pharmacia Biotech, Piscataway, NJ), purified by HPLC by means of a 301VHP575P anion-exchange column (Vydac, Hesperia, CA) and a gradient of 0.1–0.25 M NaCl and 10 mM Tris (pH 8.0) over 30 min, and ethanol-precipitated. Purification of these molecules by PAGE was found to reduce their catalytic activity.

Identification of Cleavage Products. A multiple-turnover reaction was carried out in a mixture containing 20 pmol enzyme, 200 pmol substrate, 10 μ M ZnSO₄, 1 mM MgCl₂, 150 mM NaCl, and 50 mM EPPS (pH 7.5), which was incubated at 37 °C for 15 min. Reaction products were desalted using a NAP-5 column, lyophilized, and redissolved in 10 μ L of H₂O and analyzed by matrix-assisted laser desorption/ionization (MALDI) mass spectrometry.

Kinetic Analysis. Unless otherwise stated, all reactions were carried out in the presence of 10 μ M ZnSO₄, 1 mM MgCl₂, 150 mM NaCl, and 50 mM EPPS (pH 7.5). The pH of the buffer solution was adjusted in reference to the final reaction mixture at 37 °C. Products were analyzed as described previously.¹⁹ *k*_{cat} and *K*_M values for reactions carried out under multiple-turnover (excess substrate) conditions and *k*_{obs} values for reactions carried out under single-turnover (excess enzyme) conditions were obtained as described previously.¹⁹

Metal and pH Dependence. The dependence of the catalytic rate on Zn²⁺ concentration was measured under single-turnover conditions employing 100 nM enzyme, 1 nM [5'-³²P]-labeled substrate, 1–100 μ M ZnCl₂, 1 mM MgCl₂, 150 mM NaCl, and 50 mM EPPS (pH 7.5) at 37 °C. The dependence on pH was measured under single-turnover conditions employing either 100 or 400 nM enzyme, 1 nM [5'-³²P]-labeled substrate, 10 μ M ZnCl₂, 1 mM MgCl₂, 150 mM NaCl, and 50 mM buffer (pH 5.9–8.2) at 37 °C. The pH range for reactions buffered by 2-[*N*-morpholino]-ethanesulfonic acid (MES) was 5.9–6.7, by 1,4-piperazinediethanesulfonic acid (PIPES) was 6.6–7.6, and by EPPS was 7.5–8.2. The dependence of the catalytic rate on the identity of the divalent metal ion was determined by employing 100 nM enzyme, 1 nM [5'-³²P]-labeled substrate, 0.1–10 mM divalent metal cation, 150 mM NaCl, and 50 mM EPPS (pH 7.5) at 37 °C.

Results

In Vitro Selection. A library of approximately 10¹⁵ different imidazole-containing DNA molecules was constructed, replacing thymidylate with the C5-imidazole derivative of deoxyuridylate shown in Figure 1A. The imidazole-containing analogue was incorporated as a deoxynucleoside 5'-triphosphate by a primer extension reaction employing reverse transcriptase as a DNA-dependent DNA polymerase. The primer contained a 5'-biotin moiety, followed (in a 5'→3' direction) by a short oligodeoxynucleotide spacer and 12 potentially cleavable ribonucleotides. It was hybridized to the 3' end of a DNA template that contained 50 random deoxynucleotides and 15 deoxynucleotides of defined sequence at both the 3' and 5' ends. Following primer extension, the resulting double-stranded molecules were attached to a streptavidin solid support and the non-biotinylated strand was removed by brief washing with 0.1 N NaOH. The remaining imidazole-containing single-stranded DNA molecules (Figure 1B) were challenged to cleave one of the phosphodiester linkages within the attached RNA substrate, thereby becoming detached from the support. The reaction conditions were chosen to resemble those of a living cell, employing 10 μ M Zn²⁺, 2 mM Mg²⁺, and 150 mM Na⁺ at pH 7.5 and 37 °C. The released molecules were recovered and amplified by PCR, using the fixed regions surrounding the random region as primer binding sites. The PCR products were used to construct a new population that was enriched with catalytically active molecules.

A total of 16 rounds of selective amplification were performed to obtain the best catalysts. During the first seven rounds, the

Clone	Sequence	Activity
16.2-3*	5'- CCGAGGCACCAATC CTTCGTTGAGCTCT-TACTCGG TGAAACGCCGCTA -3'	++
16.2-11	5'- CCCAGAAGGCCGAAACCG CTTCGTTGACCCCT-TGCTCTA GGGTTACTAGG -3'	++++
16.2-12*	5'- GACAGCAATAT CTTCGTTGACCCCT-TGCTCTA TATAGCCTTCAGGCCCCC -3'	++
16.3-4*	5'- CACACGGGACGCATCGGA CTTCGTTGAGCACT-TACTCTA GCCGCGCCCAT -3'	+++
16.4-3*	5'- CCACACCGTACACCAGCT CGAGGTTGGGCACC-TACTCTA ACACCAGCGGT -3'	+
16.4-4	5'- GGGACAATGGCCATTAGCCC CTTCGTTGAGCAGCTACACTA GGCCCA -3'	++

Figure 2. Sequence of the variable region of a typical clone from each of the six families obtained following the 16th round of in vitro selection. Asterisks indicate families that also were identified within the populations obtained following rounds 8 and 10. T corresponds to a position occupied by imidazole-dU. The box indicates the region of high sequence similarity present in all six families. Activity corresponds to the relative rate of self-cleavage in the presence of 10 μM Zn^{2+} .

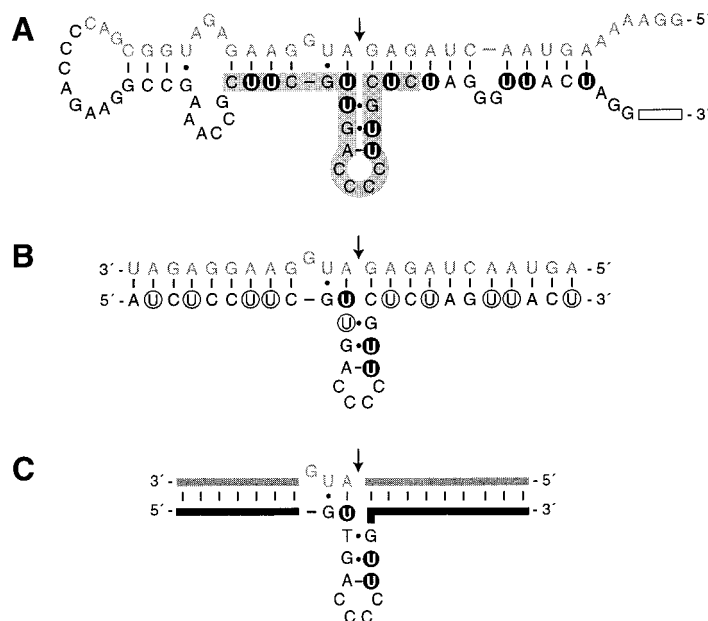


Figure 3. Structure of the 16.2-11 imidazole-functionalized DNA enzyme. (A) Intramolecular cleavage of an all-RNA substrate. Arrow indicates the cleavage site within the 34-nucleotide RNA domain (gray letters). Shaded area indicates nucleotides within the region of high sequence similarity. Imidazole-containing residues are highlighted by a black circle. Fixed primer binding site is indicated by an open rectangle at the 3' end. (B) Intermolecular cleavage with extended base-pairing. Essential imidazole-containing residues are indicated by a black circle; those that could be replaced by thymidylate are indicated by a white circle. (C) Minimal composition of the 16.2-11 enzyme. Thick gray and black lines correspond to ribo- and deoxyribonucleotides, respectively, of any complementary sequence.

reaction time was 1 h. To increase the stringency of selection, the reaction time was decreased to 30 min for round 8 and to 1 min for rounds 9 and 10. Assays of the catalytic activity of populations obtained following rounds 8 and 10 revealed three preferred cleavage sites within the 12-nucleotide RNA substrate domain (Figure 1B). Individual molecules were cloned from the population following the 8th and 10th rounds and were sequenced. Several distinct families were identified, each appearing to have been derived from a single founder molecule. Some, but not all, of the cloned individuals were able to cleave an attached RNA substrate that was surrounded by RNA rather than DNA nucleotides.

The population of molecules obtained following the 10th round of in vitro selection was divided into four lineages, two that were randomly mutagenized prior to the 11th and 14th rounds and two that were not. Of the two mutagenized and non-mutagenized lineages, one was allowed to react in the presence of 1 μM Zn^{2+} and the other in the presence of 10 μM Zn^{2+} . During the last 6 rounds of selection, the molecules were required to react in solution, cleaving an attached all-RNA substrate. Reacted molecules were selected on the basis of their increased electrophoretic mobility in a denaturing polyacrylamide gel compared to that of unreacted molecules.

Following the 16th round of in vitro selection, the population from each of the four lineages exhibited a strong preference

for cleavage at a particular RNA phosphodiester (Figure 1B). Cloning and sequencing revealed six distinct families, four that had been identified in the population following the 8th and 10th rounds. A typical representative of each of the six families is shown in Figure 2. These individuals have a region of high sequence similarity of ~ 20 residues that is located at various positions within the formerly random domain.

Identification of the Catalytic Motif. The cloned individual that exhibited the highest level of catalytic activity was derived from the mutagenized lineage that was made to react in the presence of 10 μM Zn^{2+} . It was designated as "16.2-11", the 11th clone obtained from the second lineage following the 16th round of selection. Examination of its sequence suggested the presence of Watson-Crick pairing interactions between the DNA and RNA domains, involving nucleotides on both sides of the cleavage site (Figure 3A). In addition, there appeared to be a short hairpin structure within the DNA, located close to the cleavage site and containing four imidazole-substituted deoxyuridine residues. The sequence covariation observed among the cloned individuals supports the existence of this putative hairpin.

The sequence conservation of the region containing the hairpin structure suggested that it was necessary for the function of the 16.2-11 catalyst. Whether this region was sufficient for catalysis was not known. Deletion analyses were performed to

define the minimal catalytic motif and to test possible base-pairing interactions involving the DNA and RNA domains. A set of 3'-terminal deletion mutants was constructed by template-directed primer extension in the presence of dideoxy-CTP. This ensemble of molecules was allowed to react in the presence of 10 μM Zn^{2+} , and the products were analyzed by PAGE. The catalytically non-essential nucleotides at the 3' end were determined by identifying the smallest 3'-truncated molecule that still was capable of catalyzing the rapid cleavage of the attached RNA substrate (Figure 3A). Similarly, the non-essential nucleotides at the 5' end were determined by constructing and analyzing a series of 5'-terminal deletion mutants. Taken together, these studies revealed that the ~ 20 mer region of high sequence similarity was sufficient for robust catalytic activity in the intramolecular cleavage reaction. However, when the 20mer region was prepared as an isolated molecule and directed to cleave a separate RNA substrate, no cleavage was observed. The putative substrate-recognition domains of the catalyst then were extended by five nucleotides in the 5' direction and six nucleotides in the 3' direction, resulting in a molecule that was able to cleave a separate RNA substrate with a rate comparable to that of the intramolecular cleavage reaction (Figure 3B).

The 16.2-11 molecule with extended substrate-recognition domains contained 13 imidazole-deoxyuridine residues. It seemed likely that many of these modified residues could be replaced by thymidine without reducing catalytic activity. To identify the imidazole-deoxyuridine residues that were required for activity, it was necessary to prepare the corresponding imidazole-functionalized deoxyuridine phosphoramidite (Figure 1C). Several different forms of the 16.2-11 enzyme were synthesized, testing various combinations of either imidazole-deoxyuridine or thymidine at the 13 positions. This analysis revealed that only three imidazole-containing residues were necessary for catalysis, all located close to the cleavage site (Figure 3B). Placing imidazole-deoxyuridine residues at any combination of two of these three positions resulted in no activity, while a molecule with the three imidazole substitutions was as active as the molecule that contained all 13.

The 16.2-11 enzyme appears to form a three-helix junction involving the internal hairpin and the two substrate-recognition domains. The cleavage site is located at the junction, directly opposite from the hairpin. The hairpin contains two wobble pairs and one Watson-Crick pair and is closed by a loop of four deoxycytidine residues (Figure 3B). Changing the dT·dG wobble pair at the base of the hairpin to dC·dG reduced activity, while changing it to dT·dA did not. Changing the dG·imidazole-dU pair in the middle of the hairpin to dA·imidazole-dU reduced activity only slightly. Inserting an additional base pair at the end of the hairpin reduced activity substantially. Changing the loop sequence from CCCC to GCAC did not significantly reduce activity. The latter sequence was found to occur among many of the selected clones (Figure 2). However, changing the loop to the stable "triloop" sequence AAG abolished activity. In summary, the detailed composition of the internal hairpin strongly influences the activity of the 16.2-11 enzyme.

With the exception of the rU and rG residues located downstream from the cleavage site, the 16.2-11 enzyme appears to recognize its substrate entirely through Watson-Crick base pairing (Figure 3B). To investigate nonstandard pairing interactions involving the rU and rG residues, a number of variant enzymes and substrates were prepared by chemical synthesis and tested in the intermolecular cleavage reaction. The putative rU·dG "wobble" pair located two positions downstream from the cleavage site could not be replaced by rC·dG, rU·dA, or

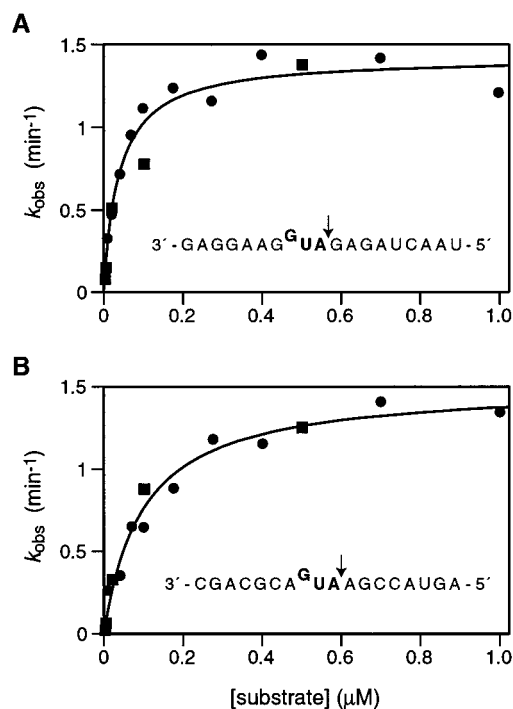


Figure 4. Catalytic activity of the 16.2-11 enzyme under multiple-turnover conditions, employing two different RNA substrates. (A) 19mer RNA substrate with a sequence corresponding to that employed during *in vitro* selection. (B) Alternative 18mer substrate in which all of the nucleotides were changed except the AUG sequence located immediately downstream from the cleavage site. Data from two independent experiments were fit a curve based on the Michaelis-Menten equation: $v = k_{\text{cat}} [\text{substrate}] / (K_{\text{M}} + [\text{substrate}])$. Reaction conditions: 10 μM Zn^{2+} , 1 mM Mg^{2+} , 150 mM Na^+ , pH 7.5, 37 °C.

rU·dT without a complete loss of catalytic activity. Similarly, the unpaired rG residue could not be deleted or changed to rA without a complete loss of activity.

The generality of the 16.2-11 enzyme with respect to the remainder of the RNA substrate sequence was tested by employing a substrate of entirely different sequence, with the exception of the AUG located immediately downstream from the cleavage site. The substrate-recognition domains of the enzyme were made complementary to the new substrate, resulting in cleavage activity comparable to that of the original enzyme-substrate combination (see below). This suggests that the imidazole-functionalized DNA enzyme can be made to cleave a wide variety of RNA substrates that contain an AUG sequence immediately downstream from the cleavage site (Figure 3C).

Properties of the Imidazole-Functionalized DNA Enzyme.

The catalytic properties of the original and sequence-modified forms of the 16.2-11 enzyme were investigated, each directed to cleave its corresponding RNA substrate (Figure 4). The substrate-recognition domains were made sufficiently short that release of the cleaved products would not limit the rate of catalytic turnover. The two enzymes were found to exhibit Michaelis-Menten saturation kinetics and operate with approximately the same catalytic rate under multiple-turnover conditions. Values for k_{cat} were 1.4 and 1.5 min⁻¹ for cleavage of the original and altered substrates, respectively (measured in the presence of 10 μM Zn^{2+} , 1 mM Mg^{2+} , and 150 mM Na^+ at pH 7.5 and 37 °C).

The catalytic rate of the 16.2-11 enzyme was independent of the concentration of Na^+ , but was highly dependent on the concentration of Zn^{2+} and on pH (Figure 5). The catalytic rate

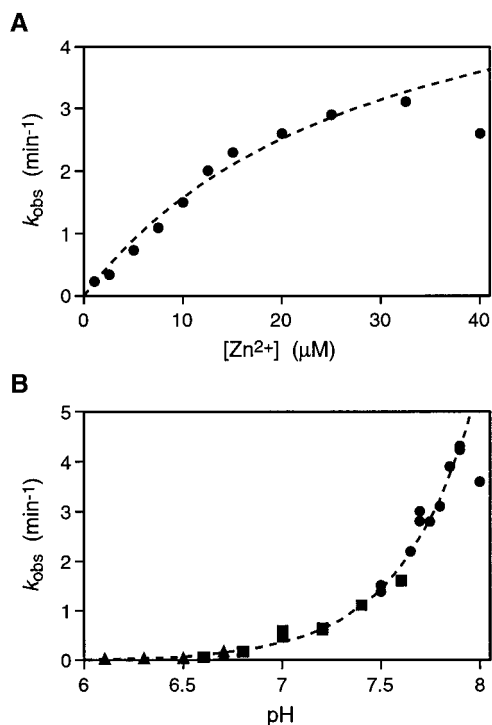


Figure 5. Dependence of the rate of substrate cleavage on reaction conditions. (A) Dependence on Zn^{2+} concentration, measured at pH 7.5. Dashed curve represents the best fit to the data for 1–32 μM ZnCl_2 , based on the equation $k_{\text{obs}} = k_{\text{max}}[\text{Zn}^{2+}]/([\text{Zn}^{2+}] + K_d)$, where k_{max} is k_{obs} in the presence of saturating Zn^{2+} and K_d is the apparent dissociation constant for Zn^{2+} . (B) Dependence on pH, measured in the presence of 10 μM ZnCl_2 . The buffer was either MES (triangles), PIPES (squares), or EPPS (circles). The dashed curve represents the best fit to the data for pH 5.9–7.9, based on the equation $k_{\text{obs}} = k_{\text{max}} K_a / (K_a + [\text{H}^+])$, where k_{max} is the limit of the catalytic rate as $[\text{H}^+]$ approaches zero and K_a is the apparent equilibrium ionization constant for a catalytically essential group.

increased with increasing Zn^{2+} concentration, reaching a maximum of 3.1 min^{-1} in the presence of 30 μM Zn^{2+} at pH 7.5. Further increases in the concentration of Zn^{2+} resulted in decreased catalytic activity, suggesting that Zn^{2+} may be inhibitory when bound at one or more low-affinity sites within the enzyme–substrate complex. Repeating this analysis at pH 6.5 did not alleviate the decrease in catalytic activity observed in the presence of high concentrations of Zn^{2+} . The catalytic rate increased exponentially with increasing pH over the range of 5.9–7.9, reaching a maximum of 4.3 min^{-1} at pH 7.9 in the presence of 10 μM Zn^{2+} (Figure 5B). Further increases in pH resulted in a steep drop in catalytic activity, perhaps due to reduced solubility of the metal ion at high pH. These results indicate that the apparent $\text{p}K_a$ of a catalytically essential group within the active site of the enzyme is ≥ 7.6 . Because the pH-rate profile does not reach a plateau before dropping off, the $\text{p}K_a$ cannot be determined accurately. The best-fit titration curve for the data up to pH 7.9 suggests that the $\text{p}K_a$ of the essential group is considerably greater than 7.6.

The ability of other divalent metal cations to support catalysis by the 16.2-11 enzyme was investigated under single-turnover conditions, employing each of the following divalent metal cations (listed in order of activity): Cd^{2+} , Mn^{2+} , Mg^{2+} , Sr^{2+} , Co^{2+} , Ca^{2+} , Ba^{2+} , Cu^{2+} , and Ni^{2+} . Catalytic activity in the presence of Cd^{2+} , Mn^{2+} , or Mg^{2+} was about 100-, 500-, and 1000-fold reduced, respectively, compared to activity in the presence of Zn^{2+} (data not shown).

The products of RNA cleavage by the 16.2-11 enzyme were

analyzed by PAGE and MALDI mass spectrometry. The electrophoretic mobility of the 5' cleavage product confirmed the presence of a terminal 2',3'-cyclic phosphate, based on comparison with authentic material produced by partial alkaline hydrolysis of the substrate RNA (data not shown). The 5' and 3' cleavage products had observed masses of 3925 and 4265 D, respectively, identical to those calculated for products terminating in a 2',3'-cyclic phosphate and 5'-hydroxyl.

Discussion

The 16.2-11 imidazole-functionalized DNA enzyme exhibits a unique set of functional properties. Like most RNA-cleaving nucleic acid enzymes, it recognizes its RNA substrate primarily through Watson–Crick base pairing. This makes it possible for the enzyme to cleave a variety of target RNAs by simple alteration of the substrate-recognition domains. Like many protein enzymes, the 16.2-11 DNA enzyme contains essential imidazole groups that are likely to be involved in catalysis. These imidazole substituents allow the small, ~28-nucleotide enzyme to achieve a catalytic rate of $>1 \text{ min}^{-1}$ in the presence of only micromolar concentrations of a divalent metal cation.

The chemical transformation catalyzed by the imidazole-functionalized DNA enzyme is identical to that catalyzed by many small nucleic acid enzymes and ribonuclease proteins. However, the detailed mechanism of catalysis may be unique among known endoribonucleases. As with other nucleic acid enzymes, the reaction rate depends on pH and the concentration of a required divalent metal ion. The enzyme is most active in the presence of Zn^{2+} but also is active with several other divalent metal cations. The order of activity for the various metals corresponds roughly to the inverse order of the $\text{p}K_a$ values of the respective metal hydrates. Taken together, these data suggest that the enzyme may utilize a tightly bound Zn^{2+} ion to activate the 2'-hydroxyl group at the cleavage site for attack on the adjacent phosphorus, resulting in RNA cleavage.

The catalytic rate of the 16.2-11 enzyme increases exponentially with increasing pH over the range of 5.9–7.9. This may reflect deprotonation of a catalytically essential group within the enzyme–substrate complex, which would imply that the catalytic rate reflects the rate of the chemical step of the reaction. Alternatively, the observed pH dependence may reflect a conformational change that perturbs the active site of the enzyme. Assuming that the observed pH dependence does reflect titration of a catalytically essential group, it is unlikely that this group is an imidazole residue functioning as a general base. The apparent $\text{p}K_a$ of this group is ≥ 7.6 , which is considerably higher than that of 4-imidazoleacrylic acid ($\text{p}K_a = 6.1$)³³ or histidine ($\text{p}K_a = 6.4$).³⁴ There is precedent for substantial $\text{p}K_a$ shifts within proteins³⁴ and structured RNAs,^{35,36} and an upward shift in the $\text{p}K_a$ of an imidazole group within the 16.2-11 enzyme as a result of electrostatic effects might be expected given the polyanionic nature of DNA. However, there is no evidence to either support or refute such a shift within the active site of the 16.2-11 enzyme. Furthermore, the value of 7.6 is a lower limit for the apparent $\text{p}K_a$ of the catalytically essential group.

The requirement for three imidazole-containing deoxyuridine analogues suggests that one or more of the imidazole groups may be involved in binding a Zn^{2+} ion that participates in catalysis. In this way, the mechanism of the imidazole-

(33) Zimmerman, S. C.; Cramer, K. D. *J. Am. Chem. Soc.* **1988**, *110*, 5906–5908.

(34) Fersht, A. *Enzyme Structure and Mechanism*, 2nd ed.; W. H. Freeman: New York, 1985; pp 155–175.

(35) Connell, G. J.; Yarus, M. *Science* **1994**, *264*, 1137–1141.

(36) Legault, P.; Pardi, A. *J. Am. Chem. Soc.* **1997**, *119*, 6621–6628.

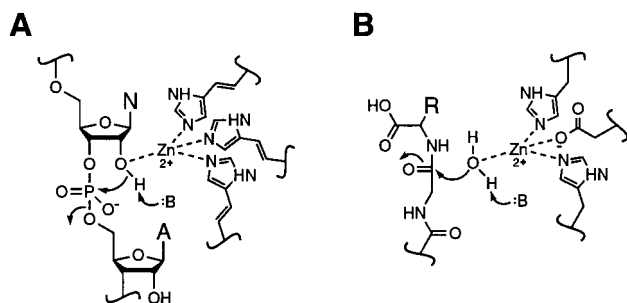


Figure 6. One possible mechanism for catalysis by the 16.2-11 DNA enzyme (A), compared to that of carboxypeptidase A (B). Both mechanisms involve an imidazole-coordinated Zn²⁺ acting as a Lewis acid cofactor.

functionalized DNA enzyme may resemble that of certain Zn²⁺-dependent protein enzymes, such as carboxypeptidase A (Figure 6).²⁸ Several alternative mechanisms for RNA cleavage by the 16.2-11 enzyme also are possible. For example, a Zn²⁺-coordinated water may act as a general base to activate the 2'-hydroxyl, or the three essential imidazole groups may play a purely structural role.

The catalytic efficiency ($k_{\text{cat}}/K_{\text{M}}$) of the 16.2-11 DNA enzyme is $\sim 10^8 \text{ M}^{-1} \text{ min}^{-1}$ under simulated physiological conditions. Like other RNA-cleaving DNA enzymes that do not contain extended chemical functionality, this value appears to be limited by the rate of RNA–DNA hybridization.¹⁹ The catalytic rate of the 16.2-11 DNA enzyme is about an order of magnitude faster than that of other nucleic acid enzymes of similar size, but about 4 orders of magnitude slower than that of RNase A. This difference may be explained in part by the advantage that protein enzymes have in positioning a greater number of functional groups near the active site.¹ This advantage is due to the relatively more flexible backbone and roughly 4-fold smaller size of subunits within proteins compared to nucleic acids. Several catalytic residues at the active site of RNase A, including two histidines, a lysine, and an aspartate, function in concert to perform the cleavage reaction.³⁷ Nucleic acid enzymes, even those endowed with enhanced functionality such as the 16.2-11 enzyme, may not be able to match protein enzymes in achieving a high density of functional groups.

(37) Raines, R. T. *Chem. Rev.* **1998**, *98*, 1045–1065.

The difference in rate enhancement between RNase A and the 16.2-11 enzyme may also be explained in part by the advantage that protein enzymes have in forming a rigid active site.¹ Rigidity is important because it allows the catalytic groups involved in stabilizing the transition state to be positioned with high effective concentration. Because RNase A has a greater density, diversity, and total number of functional groups, it may be able to achieve a higher degree of structural rigidity compared to the 16.2-11 enzyme.

Although the catalytic rate of the imidazole-functionalized DNA enzyme is inferior to that of RNase A, it was sufficient to meet the challenge imposed by the *in vitro* selection constraints. During the first seven rounds of selection, the enzyme was allowed 1 h to carry out RNA cleavage in the presence of $10 \mu\text{M Zn}^{2+}$. Under those conditions, there was no pressure favoring the selection of a larger, faster enzyme. Furthermore, because small catalysts such as the 16.2-11 enzyme were present in higher copy number in the initial pool compared to larger motifs, these small catalysts had an initial advantage. It is possible that an imidazole-functionalized DNA enzyme of larger size and with catalytic properties more closely resembling those of RNase A might have been obtained if more stringent conditions had been applied during the early rounds of *in vitro* selection.

The development of the 16.2-11 DNA enzyme demonstrates how the mechanistic properties of DNA and protein enzymes can be combined in a single molecule. This was accomplished using a nucleotide analogue containing a functional group that often plays an important role in protein-based catalysis. Future studies may lead to the development of modified nucleic acid enzymes that contain chemical substituents not found in protein enzymes.

Acknowledgment. This work was supported by Johnson & Johnson Research (G.J.), NIH Grant No. CA27489 (C.B.), The Skaggs Institute for Chemical Biology (C.B. and G.J.), and a fellowship from the Corbin Foundation for Molecular Biology Research (S.S.). We thank Martha Fedor, Olke Uhlenbeck, James Williamson, and Ian Wilson for helpful comments on this work as presented in the doctoral dissertation of S.S.